Varying Joint Patterns and Compensatory Strategies Can Lead to the Same Functional Gait Outcomes: A Case Study

Tomislav Bacek[1*], Mingrui Sun[1], Hengchang Liu[1], Zhongxiang Chen[2], Dana Kulić[2], Denny Oetomo[1] and Ying Tan[1]

Abstract— This paper analyses joint-space walking mechanisms and redundancies in delivering functional gait outcomes. Multiple biomechanical measures are analysed for two healthy male adults who participated in a multi-factorial study and walked during three sessions. Both participants employed varying intra- and inter-personal compensatory strategies (e.g., vaulting, hip hiking) across walking conditions and exhibited notable gait pattern alterations while keeping task-space (functional) gait parameters invariant. They also preferred various levels of asymmetric step length but kept their symmetric step time consistent and cadence-invariant during free walking. The results demonstrate the importance of an individualised approach and the need for a paradigm shift from functional (task-space) to joint-space gait analysis in attending to (a)typical gaits and delivering human-centred human-robot interaction.

I. INTRODUCTION

Human walking has been characterised by well-established patterns [1] believed to be strongly related to the gait economy [2]. However, much remains unknown about seemingly hierarchical [3] walking mechanisms on an individual level due to the large inter/intra-person variability [1], [4]. Understanding individual gait variations is crucial for enabling effective physical human-robot interaction (pHRI). This paper presents preliminary results of an extensive human study designed to address this major gap.

Healthy adults have been reported to walk at *their optimal* spatio-temporal gait symmetries [5] and step lengths [6] and can continuously optimise their gait [7]. This has been exploited in the *assistance-facilitated adaptation* (AFA) approach [8]–[10]. In these works, a measured functional human performance (i.e., metabolic efficiency) was used to tune robotic input to improve that same performance within pHRI. Despite positive outcomes, the AFA approach is limited to non-clinical environments (e.g., power augmentation and assistance [12]) as it does not consider gait quality (i.e., joint space) and its benefits vanish when pHRI ends [11].

A different approach – *assistance-induced (motor) learning* (AIL), is needed in rehabilitation, where the goal is to evoke long-term motor changes that remain even after pHRI ends. To achieve this, both human and robot need to be optimised (over time), as proposed by the co-adaptation paradigm [13]. However, optimising walking (to induce motor learning) is particularly challenging in the patient population. Hemiparetic patients tend to experience gait symmetry as an energetic penalty [14], which forces them to maintain asymmetry [15] and walk at not the most efficient speeds [14], [16]. Furthermore, the complexities and uniqueness of compensatory strategies [17] often lead to more effortfull and less stable walking [18], [19]. This often limits conventional physical therapy, and consequently, a robot-assisted one, to focus on functional (task space – e.g., metabolic cost, gait speed) rather than quality (joint space – e.g., gait trajectory) aspects of walking. As a result, robot-assisted gait therapy is yet to show clear benefits over traditional approaches [20].

Despite seemingly different mechanisms in healthy and patient gait, some research suggests separation of the effects of speed and compensatory walking [15], [16], similar to the effects of speed in healthy cohorts [21]. Other research [22], [23] suggests that hierarchical organisation of gait parameters driving impaired gait can be studied outside the patient population provided relevant walking constraints are in place. If true, this would significantly simplify efforts to gain knowledge about the overarching gait adaptations and compensatory strategies, a prerequisite for the uptake of the AIL approach and pHRI fully centred around human users.

This paper presents preliminary results of a multi-factorial human study (on gait signature and compensatory mechanisms), demonstrating the importance of an individualised approach and the need to expand from functional gait quality metrics. In full, the study will provide a wealth of (shared) experimental data (with healthy adults), with the intended use in guiding computational modelling predicting AIL outcomes in pHRI and informing the design of a follow-up study investigating compensatory strategies in the stroke population.

II. MATERIALS AND METHODS

A. Participants

Two healthy male adults with no known gait-interfering impairments were recruited for the study (P1: 84 kg, 1.8 m; P2: 85 kg, 1.78 m). Both P1 and P2 had prior experience walking on a dual-belt treadmill, but only P1 with the knee orthosis (Sec. II.D). Both participants signed the informed consent form, and the ethics committee of the University of Melbourne approved the study (2021-20623-13486-3).

B. Experimental conditions

The study builds on three multidimensional factors: (1) walking speed has slow (v_1=0.4 m/s), medium (v_2=0.8 m/s),

[1]T. Bacek, M. Sun, H. Liu, D. Oetomo and Y. Tan are with the Faculty of Engineering and Information Technology, The University of Melbourne, Parkville 3010, VIC, Australia

[2]Z. Chen and D. Kulic are with the Faculty of Engineering, Monash University, Clayton 3800, VIC, Australia.

and normal (v_3=1.25 m/s) levels; (2) impairment is binary: free (w/o constraints, c_1) and impaired (w/ constraints, c_2) walking; and step frequency changes between preferred (f_3) and two lower (f_1=$0.9f_3$, f_2=$0.95f_3$) and higher (f_4=$1.1f_3$, f_5=$1.2f_3$) frequencies. Each participant goes through all 30 (2x3x5) factor combinations. Asymmetric step frequency allows consistency across walking speeds since reducing f_3 by 20% at v_1 leads to highly imbalanced walking.

The six v_i-c_j combinations are split across two data-collection sessions/days (Sec. II.C). To avoid familiarisation to speed or impairment, multiple occurrences of the speed (e.g., $v1$-$v2$-$v1$), or consecutive occurrences of the impairment condition (e.g., $c1$-$c2$-$c2$) within a session are rejected. When extended by the requirement to avoid order-of-speed bias, the choice of speed-impairment combinations across the two sessions is uniquely determined (see Fig. 1).

Fig. 1. Example experimental conditions. The participant is randomly assigned to one impairment and one speed combination during the 1st day (blue), leaving one impairment combination for the 2nd day (green). The inverted impairment combination leaves two speed combinations available on the 2nd day (yellow). To avoid the order-of-speed bias (i.e., repeated speed) leaves only one speed combination (in green) to choose from.

C. Experimental protocol

The study is organised into multiple sessions, bouts, and conditions. The participants walk on a treadmill on three days, each corresponding to one session. The first session (Ses1) is a preparatory day, while the second (Ses2) and third (Ses3) sessions are data collection days (Fig. 2).

1) Preparatory session: This session serves to collect baseline data and for participants to get familiar with the study. They start by walking at 1.25 m/s and preferred cadence for six minutes [24], followed by two 2-minute cadence-exploration periods to determine preferred step frequency [25]. The same is repeated at 0.4 and 0.8 m/s.

The participants are then instructed to find their preferred walking speed using the staircase method [26]. In short, the treadmill speed is twice gradually increased from 0.5 and decreased from 1.8 m/s, noting the participant's comfortable speed 4x and averaging it to get their preferred speed. The whole process of finding comfortable speed and step frequency at each speed is then repeated with the orthosis.

2) Data collection sessions: Participants walk across three v_i-c_j combinations lasting 25 minutes each during two data collection sessions. A metronome guides them to follow the desired step frequency that changes every five minutes

in a randomised order. The first three minutes of each 5-min test allow participants to reach 95% of their metabolic steady-state [7] and the last two are used for data averaging. Breaks of 5-10 minutes and a 5-min resting metabolic cost (MC) measurement separate the three 25-min bouts. Due to the paper's scope, MC analysis is not presented herein.

At the start of each session, participants are fitted with retroreflective markers for motion capture, wireless electromyogram (EMG) for muscle activity, and indirect calorimetry to measure MC. Their first walk at the preferred speed for six minutes serves as a warm-up [24] and a baseline. This is followed by ten repeated motions of sitting down and two passes up and down a flight of 15 stairs to calculate the EMG normalisation factors [27].

3) Walking speeds: The 1.25 m/s is speed commonly used in tests with healthy participants [8], [28], [29] and is the preferred walking speed in young adults [1], [21]. The other two speeds allow healthy-patients comparison in the future. The 0.8 m/s is a lower boundary of the community ambulator category [30] and is typical of high-functioning hemiparetic patients [14], [31], [32]. The 0.4 m/s is an upper boundary of the household ambulator category [30] and is typical of low-functioning hemiparetic patients [31], [33], [34].

D. Unilateral orthosis

A simple orthosis is used to lock the knee and elicit compensatory gait movements. The orthosis is worn on the left leg and consists of two 3D-printed cuffs and metal bars with a double-hinge joint (Fig. 3). The cuffs come in different sizes to account for variations in the participants' leg sizes, and their relative position to the knee joint can be changed with the grooved bars to provide a better fit and comfort.

E. Data collection

The study is conducted using the Motek CAREN system located at the University of Melbourne.

1) Kinematics and GRFs: Gait data is collected using a dual-belt instrumented treadmill and 10 Vicon cameras (Vicon Motion Systems, Oxford, UK). Joint motion is collected at 100 Hz and ground reaction forces (GRFs) at 1 kHz. Each participant is fitted with a set of 26 markers (spherical, 14 mm diameter, B&L Engineering, CA, USA) bilaterally placed in the pelvic and lower-limbs segments (custom marker template, Fig. 3).

2) Muscle activity: The muscle activity of eight lower limb muscles per leg is measured using surface electromyography (sEMG) Delsys Trigno (Delsys Inc., Natick, MA, USA) system connected to Vicon for data sync purposes. The wireless Trigno Avanti sensors are placed in line with muscle fibers [35] over the Tibialis Anterior (TA), Gastrocnemius Lateralis (GL) and Medialis (GM), Vastus Lateralis (VL) and Rectus Femoris (RF), Biceps Femoris (BF) and Semitendinosus (ST), and Gluteus Maximus (GMax). The participant's skin is prepared following the SENIAM guidelines [36].

F. Data processing

All analyses are carried out using custom-written scripts in Matlab 2021a (Mathworks, Massachusetts, USA).

Session 1 (approx. 2 h, with 72 min of walking))												
Baseline measurements	**Walking at 1.25 m/s for 10 minutes**			**Walking at 0.8 (OR 0.4) m/s for 7 minutes**			**Walking at 0.4 (OR 0.8) m/s for 7 minutes**			**Finding preferred speed (staircase)**	**Walking at preferred speed for 7 minutes**	
weight, height, leg length	*6m*	*2m*	*2m*	*3m*	*2m*	*2m*	*3m*	*2m*	*2m*	*0.5 m/s -> 1.8 m/s x2* *1.8 m/s -> 0.5 m/s x2*	*3m*	*2m*	*2m*

Session 2 and Session 3 (approx. 3.5 h, with 81 min of walking)									
Baseline MC	**Normalisation EMG**	**Baseline walking 6 min**	**Baseline MC**	**25 minute walking - Group 1**	**Baseline MC**	**25 minute walking - Group 2**	**Baseline MC**	**25 minute walking - Group 3**	**Baseline MC**
5 min standing	*Stair climbing; sit-to-stand*	*EMG, GRF, MC, markers*	*5 min standing*	*5 x 5 minutes at a fixed speed with different cadence*	*5-10 min rest + 5 min standing MC*	*5 x 5 minutes at a fixed speed with different cadence*	*5-10 min rest + 5 min standing MC*	*5 x 5 minutes at a fixed speed with different cadence*	*5-10 min rest + 5 min standing MC*

Fig. 2. Experimental protocol. *Top*: After taking their baseline measurements, participants walk at different speeds to determine their preferred cadences and comfortable speed. The self-selected cadence at either speed is an average of three values measured during the last 15 sec of a steady-state (6 or 3 min) and exploratory (2 min) blocks. During the latter, participants are guided by metronome away from their preferred frequency for 30 seconds and then left to walk as comfortable. No rest is given between the tests. The entire block is repeated twice, with and without the orthosis, totalling 72 minutes of walking (2x36). *Bottom*: Participants start data collection sessions by walking at the preferred speed for six minutes, which serves as a warm-up and a baseline. Rest periods of 5-10 min are given and resting metabolic cost is measured in standing before and after each test. Participants are warned using auditory cues about the upcoming change in step frequency to ensure they are aware of the change. Across the two sessions, participants cover five step frequencies at all three walking speeds twice – once with and once without the orthosis. Participants starting with two 25-minute bouts with the orthosis in Session 2 only have one such bout in Session 3, and vice versa. No participant walks more than 25 minutes in a single block.
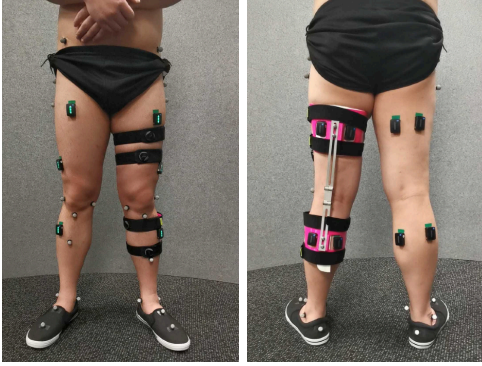

Fig. 3. A unilateral knee orthosis. The orthosis is adjustable to different leg sizes and comes with cut-outs for the EMG sensors' placement. A 4 mm thick Softair White (Massons Healthcare, VIC, Australia) padding is placed on the cuffs' inner side to improve comfort and fitting. The cuffs are held in place by four BOA straps.

1) Joint motion and GRFs: The kinematics data are filtered using a 4th order zero-lag Butterworth filter with 6 Hz cut-off frequency [1]. Lower limb joint angles are calculated from filtered 3D marker trajectories as per [37] and following ISB guidelines [38]. Data is segmented using GRFs and time-normalised to 0-100% using linear interpolation (heel strike to subsequent heel strike). The static calibration trial performed while standing at the start of each session is used as a reference for neutral joint angles [37].

2) Muscle activity: Linear envelope detection in the raw EMG data is performed using a bandpass filter (10-500 Hz) followed by a full-wave rectification and smoothening with a 200 ms moving average window. Muscle activity collected during stair climbing, sit-to-stand, and baseline walking at the start of each session are pooled and used in finding normalisation factors (per muscle per person) to avoid major drawbacks of the isometric contraction approaches [27].

G. Parameter definitions

1) Step length and time symmetry: Step length/time symmetry (Φ_T^s, Φ_L^s) is the ratio of the left leg to stride step length/time. Step length Φ_L is the fore-aft distance between the leading and trailing leg's heel marker at the time of the leading leg's heel strike. Step time Φ_T is the elapsed time between the same two events. A value of 50% marks equal Φ_T or Φ_L, while >50% a longer left Φ_T or Φ_L.

2) Hip hiking: Hip hiking is the difference between the vertical position of the anterior superior iliac spine (SIS) marker during swing and standing. When the difference is positive, a person is considered to walk with hip hiking.

3) Pelvic obliquity: Pelvic obliquity is a pelvic angle in the frontal plane. Pelvic obliquity on either leg is considered positive if the corresponding leg is lifted above the pelvic position measured in a standing trial.

III. RESULTS

1) Gait parameter symmetry: During free walking, P1 prefers asymmetric step length Φ_L and generally symmetric step time Φ_T (Fig. 4.A,B), while P2 generally walks symmetrically in both Φ_T and Φ_L (Fig. 4.C,D). Despite varying Φ_L^s (especially P1), the symmetry ratio at preferred step frequency f_{pref} at all three speeds is the same as at f_{pref} at comfortable walking speed. In general, the variability in both Φ_T^s and Φ_L^s decreases with an increase in speed.

Constraining the left knee generally reduced the constrained leg's Φ_L at 0.8 and 1.25 m/s (lower % Φ_L^s), and at multiple step frequencies also reversed the symmetry direction. A notable difference between the two participants is the effect of step frequency on Φ_L^s: higher cadence decreases the constrained leg's Φ_L in P1 and increases in P2 at 0.8 and 1.25 m/s. On the other hand, both participants increased the left leg's Φ_T during constrained walking (higher % Φ_T^s), and more so with higher walking speeds.

2) Compensatory strategies: Constrained walking caused participants to increase their hip hike (Fig. 5.I-L), albeit using different strategies. At both 0.4 and 1.25 m/s (shown here), P1 relied on his right leg's and pelvic compensatory actions to swing his left leg forward. At 0.4 m/s, P1 increased his right knee extension and decreased right ankle plantarflexion (40-60% gait, Fig. 5.A) and decreased pelvic obliquity to
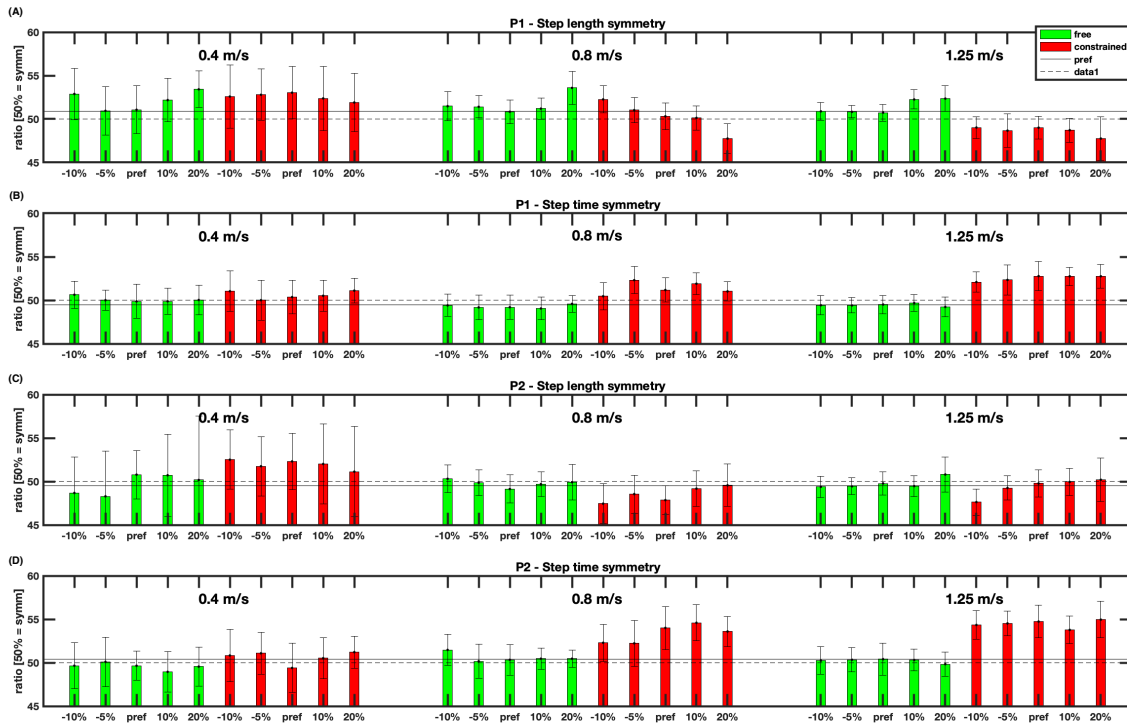
Fig. 4. Step length/time symmetry across all conditions for P1 and P2. Walking speeds are organised in columns and participants in rows (P1 in rows A and B, P2 in rows C and D). Green bars correspond to free and red bars to constrained walking. Each bar denotes a single step frequency. Bars represent the mean of the last minute of a 5-min test and error bars standard deviation. The solid horizontal line corresponds to a respective parameter value measured during preferred speed walking (P1: 1 m/s; P2: 1.05 m/s), averaged across two data collection sessions, while dashed horizontal line marks 50% value.

account for the left hip's delayed forward progression (Fig. 5.E). At 1.25 m/s, P1 exhibited no right ankle plantarflexion in mid-to-late stance (30-55% gait, Fig. 5.B) – called vaulting, to allow his constrained leg to swing forward.

On the other hand, P2 mainly relied on his right knee and pelvis to allow the constrained leg to swing forward. At 0.4 m/s (Fig. 5.C), P2 locked his right knee throughout the stance phase and increased his pelvic rotation (Fig. 5.G) to allow ground clearance. At 1.25 m/s, P2 relied on his pelvis (Fig. 5.H) and right knee extension during mid-to-late stance (Fig. 5.D) to compensate for the constrained leg, and by moving his constrained leg during swing faster (Fig. 5.H).

3) Joint-space gait alterations: Both participants exhibited changes in joint trajectories during multiple 5-min bouts (fixed v, c, and f). With no external perturbations, their knee joint (left and/or right) sometimes switched multiple times between the locked and flexed knee in the stance phase (Fig. 6.A), also seen in the knee extensor EMG activity (Fig. 6.C). However, this affected neither the anterior-posterior GRF of the relevant leg (Fig. 6.B) nor the leg's Φ_T or Φ_T^s (Fig. 6.D).

IV. DISCUSSION

In both participants and across all free walking conditions (Fig. 4), step time symmetry Φ_T^s remained largely invariant at ≈50%, similar to [5]. Step length symmetry Φ_L^s – different from [5], tended to settle over or under 50% and was affected by speed and walking f. This is notable in P1, whose Φ_L

asymmetry was minimal at f_{pref} across all three speeds, matching his preferred walking speed's Φ_L^s (black line, Fig. 4). P2 showed the same tendency at 1.25 and 0.8 m/s. A higher consistency in Φ_T^s across conditions suggests that Φ_T^s might not play as dominant a role in shaping the energetic landscape of healthy persons' walking as suggested in [39].

Constraining the left knee had both participants increase their Φ_L^s ratio at 0.4 m/s compared to free walking (i.e., longer constrained leg steps), with P1 keeping and P2 reversing his preferred asymmetry direction. This direction, opposite to what patients at comparable speeds prefer [16], is again reversed for both participants at 0.8 and 1.25 m/s. For P1, this also meant reversing his preferred Φ_L^s direction. Interestingly, increasing f at the two speeds had the opposite effects on the Φ_L^s ratio in P1 (decreasing) and P2 (increasing). On the other hand, constraining the knee led to an increase in Φ_T^s at all speeds, and more so the higher the speed. At the same time, Φ_T^s shows more consistency across f at higher walking speeds, which aligns with the theoretical importance timing of gait events has on walking energetics [2] and experimentally-validated time-invariance of key gait events during human-robot interaction [11], [44].

The identified trends in spatio-temporal gait parameters, defined in task space, do not uniquely translate into the joint space due to redundancies in the human musculoskeletal system. For example, walking free at 0.4 m/s and preferred f had P1 and P2 use different kinematics despite similar Φ_T^s and Φ_T^s. P1 walked with no hip hiking, locked knee,
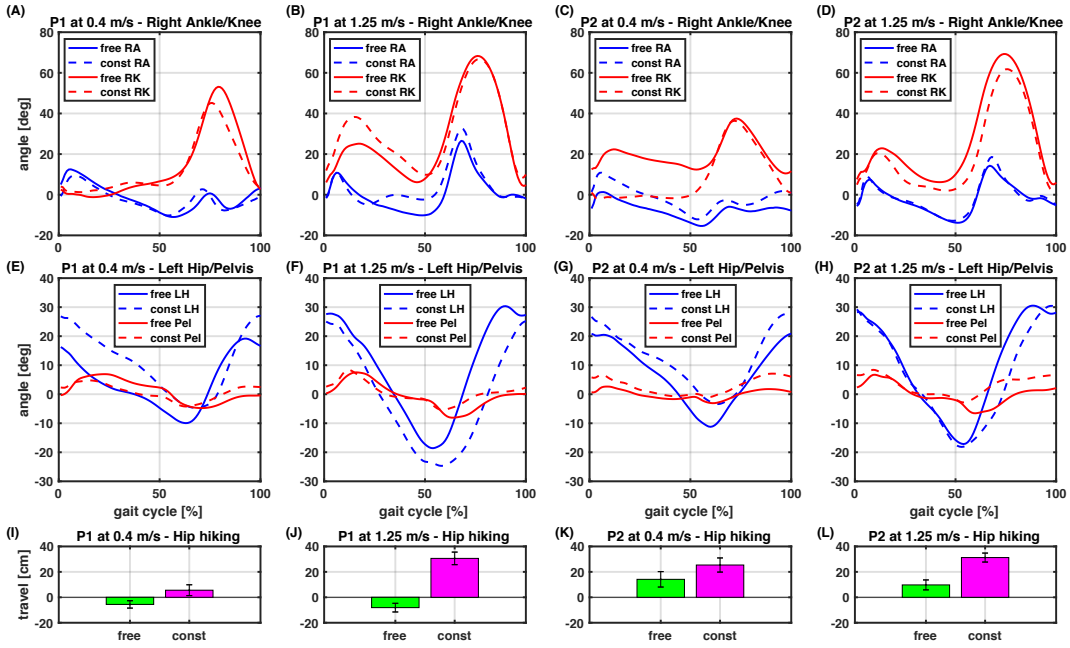
Fig. 5. Compensatory strategies during walking at 0.4 and 1.25 m/s and preferred cadence. All trajectories and bars are colour-coded across the impairment factor. The top row shows the right (unconstrained) leg's ankle and knee joint trajectories (RA = right ankle, RK = right knee), and middle row pelvis and the left (constrained) leg's hip joint trajectories (LH = left hip). The bottom row shows the participants' hip hiking. All data is an average over the last minute of walking of the respective 5-min test (standard deviation omitted for clarity purposes). Error bars in the bottom row show one standard deviation.

and high dorsiflexion (Fig. 5.A,E,I), a complete opposite to P2 (Fig. 5.C,G,K). On the other hand, their joint trajectories look similar at 1.25 m/s. Interestingly, the timing of the key gait events (e.g., ankle push-off, peak knee flexion in swing) remained remarkably consistent, in line with theoretical considerations [2] and model predictions [40], [41].

Constraining the knee increased hip hiking in both P1 and P2, albeit to a different extent (Fig. 5.I-L). Analogous to free walking, similar Φ_T^s and Φ_L^s at f_{pref} translated into different compensatory strategies. At 0.4 m/s, P1 used corrective actions at the ankle and knee joint level to compensate for delayed forward progression of the constrained leg. P2, on the other hand, relied mostly on the increased pelvic tilt and locked knee joint. This strategy of relying on the free (i.e., unimpaired) leg when $\Phi_L^s > 50\%$ is common in the patient population [43], which suggests that compensatory mechanisms may not only depend on the impairment but also the person's unique, pre-morbidity gait signature.

As Fig. 6 shows, compensatory mechanisms are not the only way humans can adjust their gait. On an intra-person level, individuals can seemingly effortlessly change their gait in the joint space (joint trajectories) while not affecting the task space performance (GRF, Φ_T^s). How these adjustments reflect in, e.g., gait energetics, remains unclear, as does why participants kept changing their joint trajectories. Invariance in GRFs and temporal gait parameters in gait trajectories points towards the preservation of the inverted pendulum dynamics [42], a mechanism found in a neurologically-impaired population [22] as well. However, the results presented in this paper demonstrate that human gait is much more complex than simple mathematical presentations and

that it can only be understood by studying it on an individual level and in both task and joint space.

V. CONCLUSIONS

This paper demonstrates through a case study that individuals do not necessarily optimise the same gait parameters and can utilise different compensatory strategies even when their spatio-temporal parameters are similar. The results also show that humans can seemingly effortlessly tap into the redundant musculoskeletal mechanisms, providing further evidence for the importance of studying both functional (task space) and quality (joint space) aspects of walking.

APPENDIX

A video (.mp4) is added to this paper, showing P1 and P2's constrained walking at 0.4 and 1.25 m/s and preferred f and demonstrating their different compensatory strategies.

ACKNOWLEDGMENT

REFERENCES

[1] D. Winter, Biomechanics and Motor Control of Human Movement, Fourth Edition. Wiley, 2009.
[2] A.D. Kuo et al., Energetic Consequences of Walking Like an Inverted Pendulum: Step-to-Step Transitions, Exerc. Sport Sci. Rev., Vol. 33(2), 2005.
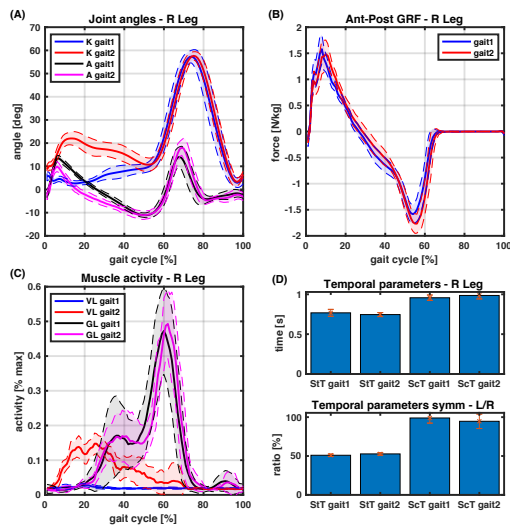
Fig. 6. Joint-space patterns within a steady-state walking (P1 at 0.8 m/s, constrained and f_{pref}). Gait1 corresponds to cycles 23-79 and Gait2 cycles 80-93 within a 5-min test. All data are averaged over noted cycles and shown for the unconstrained leg, with the shaded area representing standard deviation. (**A**) Knee (K) and ankle (A) joint angles. (**B**) Anterior-posterior GRF corresponding to gait cycles in (A). (**C**) The measured activity of GastroLat (GL) and VasLat (VL) muscles. (**D**) Step time (StT) and stance time (ScT) of the unconstrained leg (*Top*) and ratios to the left leg (*Bottom*).

[3] Y.P. Ivanenko et al., Five basic muscle activation patterns account for muscle activity during human locomotion, The Journal of Physiology, Vol. 556(1), pp. 267–282, 2004.

[4] C.A. Fukuchi et al., A public dataset of overground and treadmill walking kinematics and kinetics in healthy individuals, PeerJ, Vol. 6, 2018.

[5] E. Kodesh et al., Walking speed, unilateral leg loading, and step symmetry in young adults. Gait & posture, Vol. 35(1), pp. 66–69, 2012.

[6] J.M. Donelan et al., Mechanical and metabolic determinants of the preferred step width in human walking. Proc. R. Soc. B Biol. Sci., Vol. 268(1480), pp. 1985–1992, 2001.

[7] J.C. Selinger et al., Humans Can Continuously Optimize Energetic Cost during Walking, Curr. Biol., Vol. 25(18), pp. 2452–2456, 2015.

[8] J. Zhang et al., Human-in-the-loop optimization of exoskeleton assistance during walking, Science, Vol. 356 (6344), pp. 1280–1284, 2017.

[9] R. W. Jackson and S. H. Collins, Heuristic-Based Ankle Exoskeleton Control for Co-Adaptive Assistance of Human Locomotion, IEEE Transactions on Neural Systems and Rehabilitation Engineering, Vol. 27(10), pp. 2059–2069, 2019.

[10] D. Ye et al., Human-in-the-loop optimization of hip assistance with a soft exosuit during walking, Science Robotics, Vol. 3(15), 8p, 2018.

[11] T. Bacek et al., Human Musculoskeletal and Energetic Adaptations to Unilateral Robotic Knee Gait Assistance, IEEE Transactions on Biomedical Engineering, Vol. 69(3), pp. 1141-1150, 2022.

[12] A.J. Young and D.P. Ferris, State of the Art and Future Directions for Lower Limb Robotic Exoskeletons, IEEE Trans. Neural Syst. Rehabil. Eng., Vol. 25(2), pp. 171–182, 2017.

[13] P. Gallina et al., Progressive Co-adaptation in Human-Machine Interaction, Vol. 2, 2015.

[14] R.T. Roemmich et al., Trading Symmetry for Energy Cost During Walking in Healthy Adults and Persons Poststroke, Neurorehab. and Neural Repair, Vol. 33(8), pp. 602–613, 2019.

[15] A.L. Hsu et al., Analysis of impairments influencing gait velocity and asymmetry of hemiplegic patients after mild to moderate stroke. Archives of Phys Med and Rehab, Vol. 84(8), pp. 1185–1193, 2003.

[16] J.M. Finley and A.J. Bastian, Associations Between Foot Placement Asymmetries and Metabolic Cost of Transport in Hemiparetic Gait, Neurorehab and Neural Repair, Vol. 31(2), pp. 168–177, 2016.

[17] S.J. Ali et al., Post-stroke hemiplegic gait: A review, Pharma Innov., Vol. 3(8), pp. 36–41, 2014.

[18] D.J. Farris et al., Revisiting the mechanics and energetics of walking in individuals with chronic hemiparesis following stroke:from individual limbs to lower limb joints, J. Neuroeng. Rehabil., Vol. 12(24), 2015.

[19] P.C. Kao et al., Dynamic instability during post-stroke hemiparetic walking, Gait & posture, Vol. 40(3), pp. 457–463, 2014.

[20] J. Mehrholz et al., Electromechanical-assisted training for walking after stroke. Cochrane Database of Syst Reviews, Issue 10, 2020

[21] Fukuchi et al., Effects of walking speed on gait biomechanics in healthy participants: a systematic review and meta-analysis, Systematic Reviews, Vol. 8(153), 2019.

[22] G. Stoquart et al., The reasons why stroke patients expend so much energy to walk slowly, Gait & posture, Vol. 36(3), pp. 409–413, 2012.

[23] A. Falisse et al., Rapid predictive simulations with complex musculoskeletal models suggest that diverse healthy and pathological human gaits can emerge from similar control strategies, Journal of The Royal Society Interface, Vol. 16(157), 2019.

[24] C. Meyer et al., Familiarization with treadmill walking: How much is enough? Scientific Reports, Vol. 9(1), p. 5232, 2019.

[25] K.G. Holt et al., Predicting the minimal energy costs of human walking. Medicine and science in sports and exercise, Vol. 23(4), pp. 491–498, 1991.

[26] M.J. Chung and M.J.J. Wang, The change of gait parameters during walking at different percentage of preferred walking speed for healthy adults aged 20–60 years, Gait & Posture, Vol. 31(1), pp. 131–135, 2010.

[27] A. Ghazwan, et al., Can activities of daily living contribute to EMG normalization for gait analysis? PLOS ONE, Vol. 12(4), 2017.

[28] S.H.Collins et al., Reducing the energy cost of human walking using an unpowered exoskeleton, Nature, Vol. 522(7555), 2015.

[29] P. Malcolm et al., Bi-articular Knee-Ankle-Foot Exoskeleton Produces Higher Metabolic Cost Reduction than Weight-Matched Monoarticular Exoskeleton, p. 69, 2018.

[30] J. Perry et al., Classification of walking handicap in the stroke population, Stroke, Vol. 26(6), pp. 982–989, 1995.

[31] I. Jonkers et al., Capacity to increase walking speed is limited by impaired hip and ankle power generation in lower functioning persons post-stroke. Gait & posture, Vol. 29(1), pp. 129–137, 2009.

[32] M.D. Lewek et al., The Presence of a Paretic Propulsion Reserve During Gait in Individuals Following Stroke. Neurorehab and neural repair, Vol. 32(12), pp. 1011–1019, 2018.

[33] T.G. Hornby et al., Variable Intensive Early Walking Poststroke (VIEWS): A Randomized Controlled Trial. Neurorehab and neural repair, Vol. 30(5), pp. 440–450, 2016.

[34] G.B. Mahtani et al., Altered Sagittal- and Frontal-Plane Kinematics Following High-Intensity Stepping Training Versus Conventional Interventions in Subacute Stroke. Physical therapy, Vol. 97(3), pp. 320–329, 2017.

[35] P. Konrad, The ABC of EMG: a practical introduction to kinesiological electromyography. Noraxon USA, Inc, 2006.

[36] Seniam. [Online]. Available: http://www.seniam.org/

[37] D. Robertson et al., Research Methods in Biomechanics: Second edition (eBook), 2013.

[38] G. Wu et al., ISB recommendation on definitions of joint coordinate system of various joints for the reporting of human joint motion—part I: ankle, hip, and spine, J of Biomech, Vol. 35(4), pp. 543–548, 2002.

[39] J. Stenum and J.T. Choi, Step time asymmetry but not step length asymmetry is adapted to optimize energy cost of split-belt treadmill walking, The J of Physiology, Vol. 598(18), pp. 4063–4078, 2020.

[40] B. Koopman et al., Speed-dependent reference joint trajectory generation for robotic gait support. Journal of biomechanics, Vol. 47(6), pp. 1447–1458, 2014.

[41] F. Moissenet al., Lower limb sagittal gait kinematics can be predicted based on walking speed, gender, age and BMI. Scientific reports, Vol. 9(1), 2019.

[42] H. Geyer et al., Compliant leg behaviour explains basic dynamics of walking and running, pp. 2861–2867, 2006.

[43] J.L. Allen et al., Step length asymmetry is representative of compensatory mechanisms used in post-stroke hemiparetic walking. Gait & posture, Vol. 33(4), pp. 538–543, 2011.

[44] C. Shirota et al., Kinematic effects of inertia and friction added by a robotic knee exoskeleton after prolonged walking, in ICORR, pp. 430–434, 2017.